A. (1988) *Oncogenes 3*, 201-204.
Polakis, P. G., Snyderman, R., & Evans, T. (1989a) *Biochem. Biophys. Res. Commun. 160*, 25-32.
Polakis, P. G., Weber, R. F., Nevins, B., Didsbury, J. R., Evans, T., & Snyderman, R. (1989b) *J. Biol. Chem. 264*, 16383-16389.
Ross, E. M., & Gilman, A. G. (1977) *J. Biol. Chem. 252*, 6966-6969.
Scatchard, G. (1949) *Ann. N.Y. Acad. Sci. 51*, 660-672.
Schaffner, W., & Weissmann, C. (1973) *Anal. Biochem. 56*, 502-514.
Smigel, M. D., Northup, J. K., & Gilman, A. G. (1982) *Recent Prog. Horm. Res. 38*, 601-622.
Stryer, L., & Bourne, H. R. (1986) *Annu. Rev. Cell Biol. 2*, 391-419.
Waldo, G. L., Evans, T., Fraser, E. D., Northup, J. K., Martin, M. W., & Harden, T. K. (1987) *Biochem. J. 246*, 431-439.
Yamamoto, K., Kondo, J., Hishida, T., Teranishi, Y., & Takai, Y. (1988) *J. Biol. Chem. 263*, 9926-9932.
Yamashita, T., Yamamoto, K., Kikuchi, A., Kawata, M., Kondo, J., Hishida, T., Teranishi, Y., Shiku, H., & Takai, Y. (1988) *J. Biol. Chem. 263*, 17181-17188.

Rhodopsin-Stimulated Activation-Deactivation Cycle of Transducin: Kinetics of the Intrinsic Fluorescence Response of the α Subunit†

Pamela M. Guy, John G. Koland, and Richard A. Cerione*
Section of Biochemistry, Cell, and Molecular Biology and Department of Pharmacology, Schurman Hall, Cornell University, Ithaca, New York 14853

Received October 12, 1989; Revised Manuscript Received March 13, 1990

ABSTRACT: The intrinsic tryptophan fluorescence of the α subunit of transducin (α_T) has been shown to be sensitive to the binding of guanine nucleotides, with the fluorescence being enhanced by as much as 2-fold upon the binding of GTP or nonhydrolyzable GTP analogues [cf. Phillips and Cerione (1988) *J. Biol. Chem. 263*, 15498-15505]. In this work, we have used these fluorescence changes to analyze the kinetics for the activation (GTP binding)-deactivation (GTPase) cycle of transducin in a well-defined reconstituted phospholipid vesicle system containing purified rhodopsin and the α_T and $\beta\gamma_T$ subunits of the retinal GTP-binding protein. Both the rate and the extent of the GTP-induced fluorescence enhancement are dependent on [rhodopsin], while only the rate (and not the extent) of the GTPγS-induced enhancement is dependent on the levels of rhodopsin. Comparisons of the fluorescence enhancements elicited by GTPγS and GTP indicate that the GTPγS-induced enhancements directly reflect the GTPγS-binding event while the GTP-induced enhancements represent a composite of the GTP-binding and GTP hydrolysis events. At high [rhodopsin], the rates for GTP binding and GTPase are sufficiently different such that the GTP-induced enhancement essentially reflects GTP binding. A fluorescence decay, which always follows the GTP-induced enhancement, directly reflects the GTP hydrolytic event. The rate of the fluorescence decay matches the rate of [^{32}P]P_i production due to [γ-^{32}P]GTP hydrolysis, and the decay is immediately reversed by re-challenging with GTP. The GTP-induced fluorescence changes (i.e., the enhancement and ensuing decay) could be fit to a simple model describing the activation-deactivation cycle of transducin. The results of this modeling suggest the following points: (1) the dependency of the activation-deactivation cycle on [rhodopsin] can be described by a simple dose response profile; (2) the rate of the rhodopsin-stimulated activation of multiple α_T(GDP) molecules is dependent on [rhodopsin] and when [α_T] > [rhodopsin], the activation of the total α_T pool may be limited by the rate of dissociation of rhodopsin from the activated α_T(GTP) species; and (3) under conditions of optimal rhodopsin-α_T coupling (i.e., high [rhodopsin]), the cycle is limited by GTP hydrolysis with the rate of P_i release, or any ensuing conformational change, being at least as fast as the hydrolytic event.

Over the past several years, a number of types of receptor-coupled signal transduction systems have been identified and characterized. These include the hormone receptor systems involved in the stimulation and inhibition of adenylyl cyclase activity (Lefkowitz & Caron, 1988), the rhodopsin-mediated stimulation of a visual signal (Stryer et al., 1981; Fung, 1983), and the receptor-mediated regulations of phospholipase C (Smith et al., 1986; Berridge, 1987), phospholipase A_2 (Burch et al., 1986), and ion channels (Hescheler et al., 1987; Logothetis et al., 1987; Yatani et al., 1987). In most of these cases, three membrane-associated proteins are responsible for the change in the levels of a second messenger compound (e.g., cyclic AMP, cyclic GMP, Ca^{2+}, etc.) that is essential for the biological response. These proteins include the cell surface receptor itself, a GTP-binding protein (G protein) which serves as a signal transducer, and the biological effector (enzyme or ion channel) that is directly responsible for altering the levels of a specific second messenger.

The vertebrate vision system offers an especially attractive model for studying the regulatory interactions of a cell surface receptor with a G protein, or the ensuing interactions of the

† This research was supported by grants from the National Institutes of Health (EY06429 and GM40654), the Pew Biomedical Research Scholars Program, and the Cornell Biotechnology Program, which is supported by the New York State Science and Technology Foundation, a consortium of industries, and the United States Army. P.M.G. was supported by National Institutes of Health Research Service Award 5T32GM07272.

* To whom correspondence should be addressed at the Department of Pharmacology, Cornell University.

0006-2960/90/0429-6954$02.50/0

G protein with its biological effector, since milligram quantities of each of the primary components can be purified from rod outer segments. These protein components include the photoreceptor rhodopsin, the GTP-binding protein transducin, and the effector enzyme cyclic GMP phosphodiesterase. Rhodopsin is a single-chain glycoprotein of M_r 37 000 (Hargrave et al., 1983). Its primary amino acid sequence suggests a structure similar to that of the α_2- and β-adrenergic receptors (Kobilka et al., 1987; Dixon et al., 1986) and the different members of the muscarinic acetylcholine receptor family (Kubo et al., 1986a,b). The GTP-binding protein transducin shares the general structural features of a number of other members of the G-protein family [cf. Gilman (1987)]. It is a heterotrimeric protein with the subunits being designated as α_T (M_r = 39 000), β (M_r = 36 000), and γ_T (M_r = 5000–10 000) [cf. Fung (1983)]. The effector enzyme operating in visual transduction, the cyclic GMP phosphodiesterase (PDE), does not show strong homology with any other known signaling effector protein. Like transducin, the PDE also consists of three types of polypeptide chains. These are designated as α (M_r = 85 000–88 000), β (M_r = 85 000–88 000), and γ (M_r = 14 000) (Baehr et al., 1979; Kohnken et al., 1981).

It has been commonly proposed that the light activation of rhodopsin promotes its interaction with transducin and that this interaction catalyzes the exchange of a tightly bound GDP molecule on the α_T subunit for GTP (i.e., the activation event). The GTP-bound α_T subunit is then thought to dissociate from the photoreceptor and the $\beta\gamma_T$ subunit complex and interact with the PDE, thereby catalyzing the hydrolysis of cyclic GMP. The α_T(GTP)-stimulated PDE activity persists until the bound GTP molecule is hydrolyzed to GDP. This GTPase event signals the deactivation of transducin and provides a mechanism for the signaling cycle to return to its starting point.

The assumption is that all receptor–G-protein-coupled signaling systems will operate via a similar set of events. Despite the fact that we have a solid understanding of the protein components involved in the rhodopsin-mediated visual response, and of the general scheme by which this response occurs, the mechanistic details underlying the receptor-stimulated activation of the G protein, or the G-protein-mediated stimulation of the effector enzyme, have not yet been fully delineated. Various approaches have been used for studying the kinetics of the activation and deactivation steps of the retinal G protein which include measurements of [^{35}S]GTPγS binding (Wessling-Resnick & Johnson, 1987a,b), [γ-^{32}P]GTP hydrolysis (Fung, 1983), and light-scattering changes [Bennett & Dupont, 1985; also cf. Chabre (1985)]. However, the radioisotopic measurements do not provide for a continuous assay system in real time, while the light-scattering changes obtained from rod outer segments can be correlated with just two of the events in the activation–deactivation cycle of the G protein, specifically, the formation of the receptor–G-protein complex and the ultimate breakdown of that complex [cf. Bennett and DuPont (1985)]. Recently it was reported by Higashijima et al. (1987a,b) that changes in the intrinsic tryptophan fluorescence of the α subunits of the G_o and G_i proteins accompany the binding of different guanine nucleotides to these proteins. We subsequently demonstrated that similar changes in the intrinsic fluorescence of the α_T subunit occur and that these changes could be visualized within a well-defined reconstituted system comprised of the purified photoreceptor and the purified α_T and $\beta\gamma_T$ subunit components of transducin (Phillips & Cerione, 1988). In the work presented here, we provide evidence that the rhodopsin- and GTP-induced enhancement of the α_T fluorescence, and the ensuing fluorescence decay, accurately reflect the activation (GTP binding) and deactivation (GTPase) steps of transducin. We have begun to utilize these fluorescence changes to obtain the kinetic parameters describing the rhodpsin-stimulated GTP-binding–GTPase cycle of transducin and, in particular, to examine how rhodopsin influences these different parameters. The results of the present studies indicate that a simple model can predict the rhodopsin-stimulated activation and deactivation of transducin. Our results suggest that under some conditions the dissociation of rhodopsin from an activated α_T species may limit the rate of activation of the total α_T pool; however, the rhodopsin–α_T(GTP) complex dissociates well before GTP hydrolysis, and thus rhodopsin does not directly influence the deactivation event. The results also indicate that GTP hydrolysis, rather than product (P_i or GDP) release or any ensuing conformation change, limits the rate of the deactivation step.

Materials and Methods

Materials. Dark-adapted bovine retina were purchased from Hormel Meat Packers, Extracti-gel D was from Pierce Chemical Co., and Blue Sepharose was from Pharmacia LKB Biotechnology Inc. Concanavalin A–Sepharose, 3-[(3-cholamidopropyl)dimethylammonio]-1-propanesulfonate (CHAPS), dithiothreitol (DTT), methyl-α-mannoside, guanosine 5′-triphosphate (GTP), and soybean phosphatidylcholine (type II-S) were from Sigma Chemical Co. Guanosine 5′-*O*-(3-thiotriphosphate) (GTPγS) was purchased from Boehringer Mannheim. Octyl β-D-glucopyranoside (octyl glucoside) was obtained from Calbiochem. [γ-^{32}P]GTP and [^{35}S]GTPγS were from Dupont New England Nuclear.

Isolation of Rhodopsin and Transducin. Rod outer segments (ROS) were purified in the dark (under dim red light) essentially as described by Gierschik et al. (1984). The purified ROS were suspended in 10 mM NaHEPES (pH 7.5), 1 mM DTT, 5 mM $MgCl_2$, 0.1 mM EDTA, 100 mM NaCl, and 0.3 mM phenylmethanesulfonyl fluoride (isotonic buffer), washed several times by brief centrifugation, and then exposed to room light for 30 min. The membranes were then pelleted by centrifugation at 46000*g* for 10 min, and the pellet was resuspended in 10 mM NaHEPES (pH 7.5), 1 mM DTT, 0.1 mM EDTA, and 0.3 mM phenylmethanesulfonyl fluoride (hypotonic buffer). After several washes (performed by repeated centrifugation and resuspension of the pellet), holotransducin was eluted with the illuminated ROS membranes by resuspending the pellet in the hypotonic buffer, containing 100 μM GTP, and incubating these membranes for 30 min in room light (at 0 °C). The membranes were then pelleted and resuspended a number of times (usually at least 3), and the supernatants were combined. The pooled supernatant protein, which represents highly purified holotransducin (2–10 mg per 300 retina), was concentrated (usually about 10-fold) in an Amicon ultrafiltration cell (YM 10 membranes).

The α_T and $\beta\gamma_T$ subunit complexes of holotransducin were then purified by Blue Sepharose chromatography (Pines et al., 1985). Specifically, the concentrated holotransducin (2–10 mg) was applied to a 50-mL Blue Sepharose column that was preequilibrated with 10 mM NaHEPES (pH 7.5), 6 mM $MgCl_2$, 1 mM DTT, and 25% glycerol. The $\beta\gamma_T$ subunit complex was eluted from this column by washing with 200 mL of the above buffer. The α_T subunit complex was then eluted from the Blue Sepharose with the same buffer supplemented with 0.5 M KCl. The α_T subunit, prepared in this manner, was shown to still contain stoichiometric amounts of tightly bound GDP (the bound GDP is the outcome of the hydrolysis of the GTP initially used to elute the holotransducin from the

ROS). Thus, unless otherwise designated, the α_T subunits used in these studies are assumed to contain bound GDP. The α_T and $\beta\gamma_T$ subunit complexes were stored at −70 °C.

Rod outer segments, which were isotonically and hypotonically washed as outlined above, were used to purify rhodopsin by the procedure of Litman (1982) with the exception that 10 mM CHAPS was substituted for octyl glucoside. Specifically, the washed ROS were suspended in 50 mM Tris–acetate (pH 7.0), 1 mM $CaCl_2$, 1 mM $MnCl_2$, 0.15 M NaCl, and 10 mM CHAPS, the suspension was centrifuged at 100000*g* for 60 min, and the supernatant (containing the solubilized rhodopsin) was collected. The solubilized rhodopsin was then applied to a 10-mL concanavalin A–Sepharose column, which was preequilibrated in the above Tris–acetate/CHAPS buffer, and the protein was eluted with 0.1 M methyl α-mannoside. The eluted protein, which represents highly purified rhodopsin (90%), was stored at −70 °C.

Preparation of Rhodopsin-Containing Phosphatidylcholine Vesicles. The incorporation of purified rhodopsin into phosphatidylcholine vesicles was typically performed as follows. Soybean phosphatidylcholine (Sigma, type II-S; 50 μL of a 17 mg/mL sonicated solution) was incubated with 25 μL of octyl glucoside (17%) and 225–325 μL of 10 mM NaHEPES (pH 7.5), 100 mM NaCl, 1 mM DTT, and 5 mM $MgCl_2$ for 30–45 min on ice. The purified rhodopsin (100–200 μL from a stock solution containing 30 μM rhodopsin) was then added to the lipid/octyl glucoside mixture in the dark, and then the entire mixture (500-μL total volume) was applied to a 1-mL column of Extracti-gel resin. Prior to the addition of the reconstitution mixture, the Extracti-gel resin was preequilibrated with 10 mM NaHEPES (pH 7.5), 100 mM NaCl, and 2 mg/mL bovine serum albumin and then equilibrated with 10 mM NaHEPES (pH 7.5), 100 mM NaCl, 1 mM DTT, and 5 mM $MgCl_2$ (vesicle elution buffer). The rhodopsin-containing lipid vesicles were eluted from the resin by then washing the column with 2 mL of the vesicle elution buffer.

In some cases, the incorporation of rhodopsin into lipid vesicles was performed by incubating 16 μL of soybean phosphatidylcholine with 9 μL of octyl glucoside and 75 μL of 10 mM NaHEPES (pH 7.5)/100 mM NaCl for 30 min on ice. At this point, 1–50 μL of purified rhodopsin (from a 5 μM stock solution) was added to the lipid/octyl glucoside incubation. The mixture (150 μL) was then added to 0.5 mL of dried Extracti-gel resin in a 1-mL syringe. The Extracti-gel was pretreated as described above, and the rhodopsin-containing lipid vesicles were then eluted from the resin using 250 μL of the vesicle elution buffer (yielding 400 μL of rhodopsin-containing vesicles).

The efficiencies of incorporation of rhodopsin into the lipid vesicles (54 ± 2% SE, $n = 12$) were calculated by using iodinated rhodopsin and were found to be constant over the range of rhodopsin concentrations examined in the experiments. These values were in good agreement with those previously determined (Cerione et al., 1985). The iodination of purified rhodopsin was performed using chloramine T (Greenwood et al., 1963). The specific activity of the iodinated rhodopsin preparation was 4900 cpm/pmol. The concentration of rhodopsin was measured from the absorbance at 498 nm, using the known extinction coefficient for retinal (42700 M^{-1} cm^{-1}) [cf. Litman) (1982)]. The amounts of functional rhodopsin in the different assay solutions, that are indicated in the figure legends below, were calculated by assuming that 50% of the incorporated rhodopsin molecules are properly oriented for coupling to added α_T (i.e., with their cytoplasmic domains extending from the outside of the lipid vesicles). This assumption is based on our studies using this protocol to insert different hormone receptors (the α_2- and β-adrenergic receptors) and growth factor receptors into lipid vesicles.

Reconstitution of Rhodopsin–Transducin Interactions. The interactions between light-activated rhodopsin and the purified α_T subunit were monitored by guanine nucleotide induced changes in the intrinsic fluorescence of the α_T subunit, or by measuring the light-stimulated binding of [^{35}S]GTPγS, or [γ-^{32}P]GTP hydrolysis (see below). These measurements were performed by first mixing 100–250 nM α_T subunit and 50–250 nM of the $\beta\gamma_T$ subunit complex with 8–100 nM rhodopsin in the presence of 8 mM NaHEPES (pH 7.5), 4 mM $MgCl_2$, and 0.8 mM DTT. These proteins were incubated in room light for 10 min at room temperature (i.e., conditions that were sufficient to elicit the complete conversion of the reconstituted rhodopsin to the meta II state). The assays then were initiated by the additions of GTP or GTPγS. In the experiments presented under Results, the final concentration of NaCl (or KCl) in the initial incubations and in the assay solutions varied from 20 to 60 mM; the salt was contributed from the rhodopsin-containing lipid vesicles (in 100 mM NaCl) and the α_T subunit (in 500 mM KCl). We have found that the rates for guanine nucleotide binding and the turnover numbers for GTP hydrolysis measured under these conditions were identical with those measured in experiments where the final levels of NaCl (or KCl) were fixed at 100 mM. The levels of α_T in the different assay solutions were measured by [^{35}S]GTPγS binding [see below; also cf. Cerione et al. (1985)]. For the α_T preparations used in these studies, the amount of protein determined from the [^{35}S]GTPγS binding assays was usually at least 50–60% of that measured by the Bradford (1976) assay. The amount of $\beta\gamma_T$ complex was determined by the method of Bradford, assuming a molecular weight of 45 000 for the complex.

Fluorescence Measurements. The kinetics for the rhodopsin- and GTP-induced (or GTPγS-induced) changes in the tryptophan emission of α_T were examined by first incubating rhodopsin, the α_T subunit, and the $\beta\gamma_T$ subunit complex (as described above) for 5–10 min at room temperature (and in room light) and then initiating the reaction by the addition of 2–10 μL of GTP to a final volume of 1.3 mL (which yielded the final concentrations indicated under Results). The reactants were stirred continuously in a quartz cuvette, and the fluorescence emission was monitored at 1-s intervals, using an SLM 8000 spectrofluorometer (emission = 335 nm, excitation = 280 nm). Unless otherwise noted, all fluorescence spectra were corrected for the contributions from rhodopsin and $\beta\gamma_T$.

Radiolabeled Guanine Nucleotide Binding Measurements. Assays for the rhodopsin-stimulated binding of [^{35}S]GTPγS were initiated by adding these radiolabeled guanine nucleotides to incubations containing rhodopsin, α_T, and $\beta\gamma_T$ as outlined above. At various times (5 s to 1 min), aliquots (40 μL) were removed from the binding incubations and directly added to 0.45-μm nitrocellulose filters (Schleicher & Schuell). The filters were washed twice with 10 mM NaHEPES (pH 7.5)/5 mM $MgCl_2$ and then counted in 5 mL of Liquiscint (National Diagnostics). Nonspecific binding was determined by measuring [^{35}S]GTPγS binding to rhodopsin-containing lipid vesicles in the absence of α_T. The nonspecific binding was typically <10% of the total binding.

Measurements of Rhodopsin-Stimulated GTPase Activity. The rhodopsin-stimulated GTPase activity was measured under conditions identical with those used in the fluorescence experiments and GTP-binding assays. Typically, the total assay volume was 100 μL. The assays were stopped by directly

adding an aliquot (usually 90 μL) to a solution of 10% ammonium molybdate (1 M HCl). The $[^{32}P]P_i$, generated as an outcome of GTP hydrolysis, was then quantified by a isobutanyl alcohol/benzene extraction (Avron, 1960). Identical results were obtained if the assays were first quenched by adding trichloroacetic acid (TCA, 10% final concentration) or urea (0.8 M final concentration) to the samples. This indicates that the total amount of $[^{32}P]P_i$ generated by GTP hydrolysis is in fact being measured, i.e., both the $[^{32}P]P_i$ released into the assay solution and any $[^{32}P]P_i$ that might remain associated with the α_T subunit during the time period of the assay. Apparently, any $[^{32}P]P_i$ which remains bound to α_T during the assay is subsequently released in the ammonium molybdate/HCl solution, and thus, there are no differences in the total amount of $[^{32}P]P_i$ measured when denaturants (TCA, urea) are used to quench the GTPase assay. Nonspecific hydrolysis of GTP was measured by performing identical assays in the absence of α_T and usually represented less than 1% of the total radioactivity added to the assay incubations.

Modeling of Fluorescence Enhancement Time Courses and Estimation of the Rate Constants of the Kinetic Scheme. The simplified scheme for the receptor-stimulated activation–deactivation cycle of α_T given in Figure 5B served as a framework for the analysis of the time-dependent fluorescence enhancement data and the estimation of the intrinsic kinetic constants of α_T. This scheme has a corresponding set of differential rate equations:

$$d[R\alpha(\ )]/dt = (k_{exc} + k'_{hyd})[R\alpha^*(GTP)] - k_{bind}[GTP][R\alpha(\ )]$$

$$d[R\alpha^*(GTP)]/dt = -(k_{exc} + k'_{hyd})[R\alpha^*(GTP)] + k_{bind}[GTP][R\alpha(\ )]$$

$$d[\alpha(GDP)]/dt = k_{hyd}[\alpha^*(GTP)] - k_{exc}[R\alpha^*(GTP)]$$

$$d[\alpha^*(GTP)]/dt = -k_{hyd}[\alpha^*(GTP)] + k_{exc}[R\alpha^*(GTP)]$$

$$d[GTP]/dt = -k_{bind}[GTP][R\alpha(\ )]$$

Note that k_{exc} is a first-order rate constant, which implies that the rate of exchange of an α^*(GTP) species for an α(GDP) complex on any rhodopsin molecule (R) is limited by the release of α^*(GTP) from R and not by the subsequent binding of α(GDP). It is further assumed that the dissociation of GDP from α(GDP) to form a nucleotide-depleted $\alpha(\ )$ subunit is fast. These assumptions will be considered below (Discussion). Given the initial values for the concentration of each of the species in the scheme and estimates for each rate constant, these equations were solved numerically by Euler's method [cf. McCraken and Dorn (1964)] to give a predicted time course for the buildup or decay of each of the species. With the assumption that the experimentally observed fluorescence enhancement was due solely to the formation of $R\alpha^*$(GTP) and α^*(GTP) (see below), the time course of the fluorescence enhancement could also be simulated by using the rate equation solutions. The simulated fluorescence enhancement was fit to the experimentally observed transients by a nonlinear least-squares algorithm (Nelder & Mead, 1965) with the rate constants as adjustable parameters. In this way, the best-fit values for the kinetic constants of the scheme were determined, and the simulated time courses of fluorescence enhancement were generated (see Figure 6).

A key assumption in this analysis is that the enhancement of fluorescence is coincident with the formation of those α_T species with active nucleotide bound, specifically α^*(GTP) and $R\alpha^*$(GTP), and that this enhancement is immediately reversed with the hydrolysis of the bound nucleotide. Justification for this assumption is given by the results of P_i release experiments as shown in Figure 4. If the rate of P_i release ($d[P_i]/dt$) and the time-dependent fluorescence change, $\Delta F(t)$, are both proportional to the total concentration of the activated α^*(GTP) species, then

$$d[P_i]/dt = k([\alpha^*(GTP)] + [R\alpha^*(GTP)]) = k'\Delta F(t)$$

Or upon integration:

$$[P_i](t) = k' \int_0^t \Delta F(t)\, dt$$

Hence, the integral of the transient fluorescence change predicts the time course of P_i release. In practice, the integral of the fluorescence change was approximated by a summation of the closely spaced time points. As shown in Figure 4, the rate of P_i formation predicted by integration of the fluorescence enhancement agreed very well with the rate of $[^{32}P]P_i$ formation directly assayed.

The results of steady-state kinetics assays (e.g., Figures 7 and 8) could also be simulated by these methods. In these cases, the amount of $[^{32}P]P_i$ released or $[^{35}S]GTP\gamma S$ bound in a fixed time assay was estimated by numerical solution of the corresponding differential rate equations for P_i production or $R\alpha^*(GTP\gamma S)$ and $\alpha^*(GTP\gamma S)$ formation. The production of P_i was estimated by using the rate constant values determined by fitting of the model (Figure 5B) to the fluorescence enhancement data (see above). The same rate constants values were used to estimate the binding of the nonhydrolyzable GTP analogue, except that the values of k_{hyd} and k'_{hyd} were set to zero.

Results

Fluorescence Changes Accompanying the Rhodopsin-Stimulated Activation–Deactivation Cycle of Transducin. We (Phillips & Cerione, 1988) and others (Higashijima et al., 1987a,b) have shown that when GTP or nonhydrolyzable GTP analogues are bound to the α subunits of GTP-binding proteins, the tryptophan fluorescence of these subunits is enhanced by as much as 2-fold relative to the fluorescence of α subunits which contain bound GDP. Some examples of the changes in the intrinsic tryptophan fluorescence, which accompanied the rhodopsin-stimulated activation of α_T in reconstituted phospholipid vesicle systems containing just the purified rhodopsin, the α_T subunit, and the $\beta\gamma_T$ complex, are shown in Figure 1. The addition of GTP, over a range of 20–160 nM, resulted in a rapid enhancement of the tryptophan fluorescence which can be attributed to a conformational change in the α_T subunit [cf. Phillips and Cerione (1988)]. The extents of the fluorescence enhancement were dependent on [GTP], which indicated that these enhancements were the direct outcome of the binding of GTP to the α_T subunit. However, the rates of the GTP-induced fluorescence enhancements did not appear to be influenced by [GTP] over the concentration range examined (also see Figures 6A–C, below). Following the enhancement of the tryptophan emission, there was a decay in the fluorescence which occurred over 1–2 min and returned the tryptophan emission to its initial basal level. The fluorescence decay was only elicited by GTP, and was not observed when using nonhydrolyzable GTP analogues (i.e., $GTP\gamma S$), which suggested that it reflects the deactivation event, i.e., GTP hydrolysis (see below). When $GTP\gamma S$ was substituted for GTP in these reconstituted systems, there again was an immediate enhancement in the

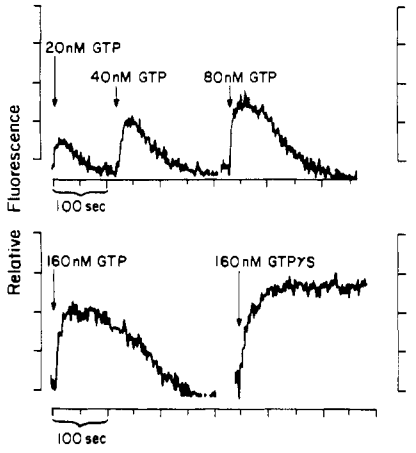

FIGURE 1: Rhodopsin- and GTP-stimulated enhancements of the fluorescence of the α_T subunit. A mixture of rhodopsin-containing phosphatidylcholine vesicles ([rhodopsin] = 30 nM), $\beta\gamma_T$ (130 nM), and α_T (200 nM) was incubated in room light for 10 min at room temperature. GTP, or GTPγS, was added to the final indicated concentrations, and the change in fluorescence emission (excitation = 280 nm, emission = 335 nm) was continuously monitored.

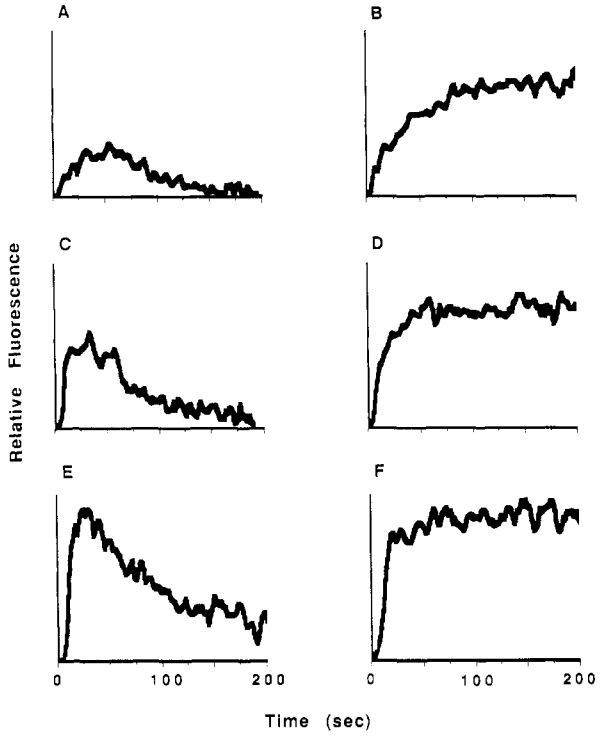

FIGURE 2: Dependence of the rhodopsin- and GTP- (or GTPγS-) stimulated fluorescence enhancements on [rhodopsin]. Rhodopsin-containing phosphatidylcholine vesicles, $\beta\gamma_T$ (130 nM), and α_T (200 nM) were incubated in room light for 10 min at room temperature. In panels A, C, and E, GTP (final concentration = 60 nM) was then added, and the change in fluorescence emission (excitation = 280 nm, emission = 335 nm) was continuously monitored. In panels B, D, and F, GTPγS was substituted for GTP. In panels A and B, [rhodopsin] = 13 nM. In panels C and D, [rhodopsin] = 30 nM. In panels E and F, [rhodopsin] = 45 nM.

tryptophan fluorescence of α_T which persisted for several minutes (Figure 1).

The results presented in Figure 2 demonstrated that the nature of the GTP- and GTPγS-induced fluorescence changes in the α_T subunit were highly dependent on [rhodopsin]. Specifically, Figure 2, panels A, C, and E, shows the GTP-stimulated fluorescence changes which occurred at varying levels of light-activated rhodopsin (i.e., 13, 30, and 45 nM); in these experiments, [GTP] = 60 nM = 0.3[α_T]. Both the

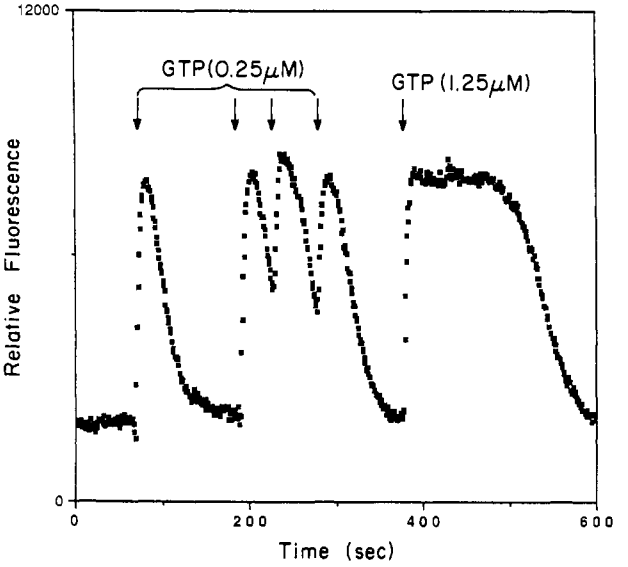

FIGURE 3: Reversibility of the GTP-induced fluorescence decay. Rhodopsin-containing phosphatidylcholine vesicles (final concentration of rhodopsin in the cuvette = 20 nM) were incubated with $\beta\gamma_T$ (250 nM) and α_T (250 nM) for 10 min in the light at room temperature. At the different time periods indicated, GTP (at the final concentrations indicated in the figure) was added, and the change in fluorescence emission was continuously monitored (excitation = 280 nm, emission = 335 nm).

rates and the extents of the GTP-induced fluorescence enhancements were dependent on [rhodopsin]. When the levels of GTP were increased, such that [GTP] $\approx$ [α_T], the rates of the GTP-induced fluorescence enhancements were still dependent on the levels of photoreceptor (for example, see Figure 6, below).

Figure 2 (panels B, D, and F) shows that the rates of the GTPγS-induced fluorescence enhancements also were dependent on the levels of rhodopsin. At high [rhodopsin], the extent of the GTPγS-induced enhancement was essentially equal to the GTP-induced enhancement (i.e., panels E and F of Figure 2). However, unlike the case for GTP, the extents of GTPγS-induced fluorescence enhancements were essentially independent of [rhodopsin]. The fact that varying [rhodopsin] did not affect the extents of the fluorescence enhancements elicited by the nonhydrolyzable GTP analogue, and only affected the extents of the GTP-induced fluorescence enhancements, suggested that the GTP-induced fluorescence changes represent a composite of the GTP-binding event and the onset of the GTP hydrolysis (which is accompanied by a fluorescence decay). This will be considered in more detail below (i.e., Figure 6).

A number of lines of evidence lead us to conclude that the fluorescence decay, which follows the rhodopsin- and GTP-induced fluorescent enhancements, in fact directly reflects GTP hydrolysis within the α_T subunit. One line of evidence came from the data shown in Figure 3 which demonstrated that the fluorescence enhancement, originally elicited by GTP, could be fully regained when the system was rechallenged with GTP. A complete restoration of the enhancement was immediately achieved when GTP was added either during the fluorescence decay or well after the decay was complete. These data suggested that the fluorescence decay cannot be significantly faster than GTP hydrolysis or the release of the hydrolysis products GDP and inorganic phosphate (P_i). For example, if the fluorescence decay were followed either by a slow GTP hydrolytic event or by a slow release of products from the α_T subunit, then there would be a lag in the onset of the new fluorescence enhancement elicited by a second challenge of

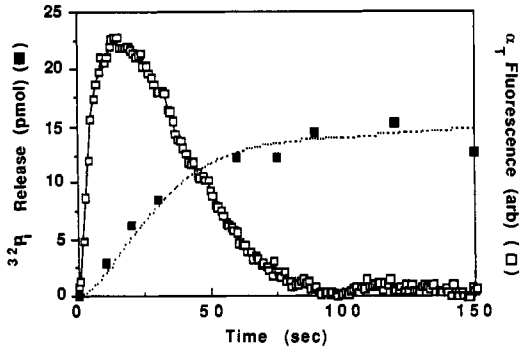

FIGURE 4: Comparisons of the rate of the rhodopsin- and GTP-induced fluorescence decay with the rate for GTP hydrolysis. Rhodopsin-containing phosphatidylcholine vesicles (final concentration of rhodopsin in the cuvette = 20 nM) were incubated with $\beta\gamma_T$ (250 nM) and α_T (250 nM) for 10 min in the light at room temperature. GTP, or [γ-^{32}P]GTP (final concentration = 300 nM in all cases), was then added to the incubation; in the former case, the fluorescence emission was continuously monitored (excitation = 280 nm, emission = 335 nm), while in the latter case [^{32}P]P_i release, as an outcome of GTPase activity, was measured (see Materials and Methods). The dotted line represents the integration of the fluorescence signal (see Materials and Methods).

GTP. This lag would reflect the time period for GTP hydrolysis or product release, since any new activation (fluorescence enhancement) event could only occur after the hydrolysis of GTP and the subsequent release of the hydrolysis products.

Under conditions of excess GTP, the fluorescence enhancement persisted for as long as 2 min (Figure 3). This also was consistent with the suggestion that the fluorescence decay directly reflected GTP hydrolysis, since high levels of GTP would cause the majority of the α_T to remain in the GTP-bound form. Eventually (after several minutes), all of the GTP was hydrolyzed and the fluorescence decayed.

The data in Figure 4 show the results of an experiment which directly compared the rates for the GTP-induced fluorescence enhancement/decay sequence and the hydrolysis of [γ-^{32}P]GTP. The integral of the time-dependent fluorescence change (dotted line) corresponded closely with the measured rate of [γ-^{32}P]GTP hydrolysis. As discussed under Material and Methods, this would be expected if the fluorescence enhancement were due to the formation of an activated GTP-bound α_T species which undergoes a first-order reaction (GTP hydrolytic event) to yield P_i. These results then verify that the GTP-induced fluorescence changes directly reflect the GTP-binding and hydrolytic events within the α_T subunits. They also require that if the release of the hydrolysis products (GDP or P_i), or a subsequent conformational change, were necessary for the decay of fluorescence, then these events must occur significantly faster than the GTP hydrolytic step.

Analysis of the Fluorescence Changes within the Context of a Simple Model for the Activation–Deactivation Cycle of Transducin. Given the fact that the GTP-induced fluorescence changes can be tightly correlated with the GTP-binding–GTP hydrolytic events, we set out to fit the fluorescence data to a simple scheme describing the rhodopsin-stimulated activation–deactivation cycle of transducin (Figure 5). The model shown in Figure 5A depicts most of the events which are generally felt to comprise a receptor-stimulated GTP-binding–GTPase cycle. It is assumed that the binding of light-activated rhodopsin (R) to an α(GDP) species first induces the release of GDP (k_{rel}), which results in a guanine nucleotide depleted α_T subunit, α( ). GTP subsequently binds to the nucleotide-depleted state (k_{bind}). This binding event is treated as a bimolecular reaction between α_T and GTP. For simplicity,

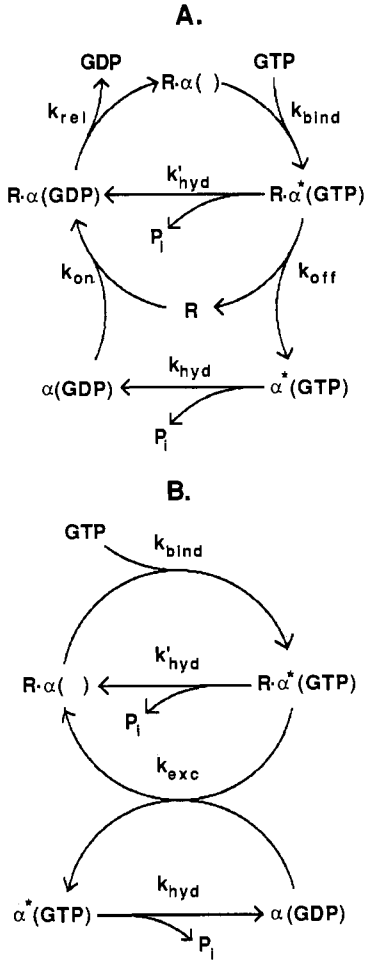

FIGURE 5: Model for the activation–deactivation cycle of the α_T subunit. (A) Scheme for the rhodopsin-stimulated GTP-binding event (activation) and the GTP hydrolysis (deactivation) occurring on the α subunit of transducin. k_{rel} represents the rate constant for the rhodopsin-stimulated GDP dissociation from α(GDP). Only the rhodopsin-coupled α(GDP) species is able to undergo guanine nucleotide (GDP–GTP) exchange over the time period of our assays [i.e., k_{rel} is extremely slow in the free α(GDP) species and thus is not shown to occur]. The GTP-binding event (k_{bind}) is assumed to be a bimolecular reaction between Rα( ), the nucleotide-depleted rhodopsin–α_T complex, and GTP which results in the conversion of α_T to an active conformation (α^*). $\beta\gamma_T$ is required for the rhodopsin-stimulated guanine nucleotide exchange in α_T; however, for simplicity, this species is not shown. k_{hyd} represents the rate constant for the hydrolysis of GTP in the free α^*(GTP) subunit, while k'_{hyd} represents the rate constant for the hydrolysis of GTP in any α^*(GTP) molecules that are still coupled to the photoreceptor. k_{off} represents the rate constant for the breakdown of the rhodopsin–α^*(GTP) complex while k_{on} represents the rate constant for the coupling of α(GDP) to rhodopsin. (B) Simplified version of the scheme shown in (A). It is based on the assumptions that $k_{rel} > k_{bind}$ [in (A)] and that $k_{off} < k_{on}$. Thus, the conversion of Rα( ) to $R\alpha^*$(GTP) is limited by the GTP-binding step (k_{bind}), and the conversion of an activated Rα^*(GTP) species to a new Rα( ) complex is limited by the release of rhodopsin (k_{exc}) from the activated α_T subunit. k_{exc} is treated as a first-order rate constant. The $R\alpha^*$(GTP) and the α^*(GTP) species are assumed to be the species responsible for the enhanced fluorescence. The fluorescence data were fit by this scheme as outlined under Materials and Methods.

the $\beta\gamma_T$ subunit complex is not shown, although it is assumed to always be bound to the rhodopsin–α(GDP) species. The binding of GTP induces an active conformation within the α_T subunit (α^*); it is this conformation which is reflected by an enhanced tryptophan fluorescence. Rhodopsin will dissociate from the α^*(GTP) species (k_{off}), since [^{35}S]GTPγS binding experiments indicate that rhodopsin can act catalytically to promote the activation of multiple α_T subunits (cf. Figure 8A,

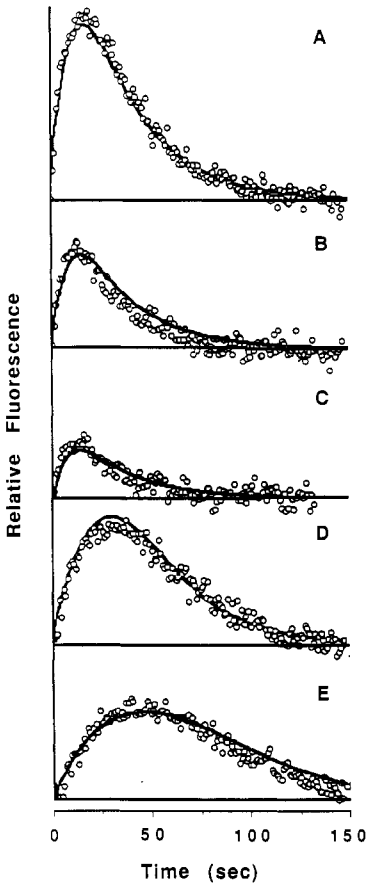

FIGURE 6: Analyses of the fluorescence data with a simple model for the activation–deactivation cycle of α_T. Rhodopsin-containing phosphatidylcholine vesicles were incubated with $\beta\gamma_T$ (final concentration = 80 nM) and α_T (150 nM) in room light for 10 min at room temperature. GTP was then added, and the change in fluorescence emission (excitation = 280 nm, emission = 335 nm) was continuously monitored. The fits to the fluorescence data with a single set of parameters values were obtained by using the model shown in Figure 5B, as described under Materials and Methods. (A) [GTP] = 170 nM, [rhodopsin] = 30 nM. (B) [GTP] = 80 nM, [rhodopsin] = 30 nM. (C) [GTP] = 42 nM, [rhodopsin] = 30 nM. (D) [GTP] = 170 nM, [rhodopsin] = 15 nM. (E) [GTP] = 170 nM, [rhodopsin] = 8 nM.

below). However, we questioned whether at increasing levels of rhodopsin the photoreceptor might be capable of staying associated with the α^*(GTP) species and directly influencing its rate of deactivation. Thus, the potential for a rhodopsin–α^*(GTP) species to deactivate and undergo GTP hydrolysis was included in the model (k'_{hyd}), as well as a deactivation step within the free α^*(GTP) species (k_{hyd}). Figure 5B shows a simplified version of the scheme depicted in Figure 5A, which allowed us to fit the fluorescence data with four (rather than six) parameters. In this version, it is assumed that the association of rhodopsin with the α(GDP) species (k_{on} in Figure 5A) is fast relative to the dissociation of rhodopsin from the α^*(GTP) complex and that the receptor-stimulated dissociation of GDP (represented by k_{rel} in Figure 5A) is fast relative to the GTP-binding step (k_{bind}) (see Discussion).

Figure 6 shows some typical fits of fluorescence data, obtained at varying levels of rhodopsin (8, 15, and 30 nM) and GTP (42, 85, and 170 nM), by the model presented in Figure 5B. Specifically, Figure 6A–C shows the fits to the data obtained at the highest level of rhodopsin (30 nM) and different levels of GTP (42–170 nM), while Figure 6D,E shows the fits to the data obtained at the highest level of GTP (170 nM) and at the two lower levels of rhodopsin (8 and 15 nM). All of the fluorescence data that we have obtained could be fit well to the simple model shown in Figure 5B, with the following ranges for the different kinetic parameters: $k_{hyd} = k'_{hyd} = 0.034–0.040\ s^{-1}$, $k_{bind} = 0.005–0.007\ nM^{-1}\ s^{-1}$, and $k_{exc} = 0.45–1.0\ s^{-1}$. Overall, these results suggest that at [GTP] $\gg$100 nM, the activation of the total α_T(GDP) pool is limited by the conversion of the α_T(GDP) species to a receptor–α_T complex. This conversion requires both the dissociation of rhodopsin from an α^*_T(GTP) molecule and the subsequent association of rhodopsin with a new α_T(GDP) molecule. The implication from the modeling is that even under conditions where both [rhodopsin] and [α_T(GDP)] are high, but with [α_T(GDP)] > [rhodopsin], the activation of multiple α_T(GDP) species by the receptor would be limited by the first-order rate constant k_{exc}, i.e., the dissociation of the photoreceptor from an activated α^*_T(GTP) species. At relatively low [rhodopsin] (i.e. [rhodopsin] < [α_T(GDP)]), the extent of the GTP-induced fluorescence enhancement would be limited by the fact that some of the α^*_T(GTP) species have begun to hydrolyze their GTP, prior to the completion of the activation of the total α_T(GDP) pool.

Similarly, these fits predict that at low levels of [GTP] (i.e., <5 nM), the rate of binding will limit the overall rate of the activation–deactivation cycle; this would probably be exaggerated by the competition between the added GTP and the GDP which was initially tightly bound to α_T. At increasing levels of rhodopsin (such that [rhodopsin] begins to approach [α_T(GDP)]) and at increasing levels of GTP (>10 nM), it is the hydrolysis of GTP which begins to limit the rate of the activation–deactivation cycle. The rate of the hydrolysis step ($0.035–0.04\ s^{-1}$) appeared to be completely independent of [rhodopsin], which suggests that the photoreceptor does not directly influence the GTPase activity of the α^*(GTP) species.

Simulations of Radiolabeled GTP-Binding and GTP Hydrolytic Data. We have examined whether the best-fit parameters obtained from the modeling of the fluorescence data can be used to simulate the data obtained from rhodopsin-stimulated [^{35}S]GTPγS binding experiments and rhodopsin-stimulated [γ-^{32}P]GTPase assays. Figure 7A shows the time courses for the rhodopsin-stimulated binding of [^{35}S]GTPγS to the α_T subunit, obtained at different rhodopsin concentrations. The rates for the binding of GTPγS to the α_T subunits were dependent on [rhodopsin], as was the case for the rates of the GTPγS-induced fluorescence enhancements. Figure 7B shows the simulated time courses that were obtained by using the best-fit parameters from the modeling of the fluorescence data. The predicted rates for the rhodopsin-stimulated binding of [^{35}S]GTPγS to α_T (Figure 7B) agree well with those experimentally determined (Figure 7A), although in some cases (particularly when [α_T] > [GTPγS]) the extent of [^{35}S]GTPγS binding which is measured experimentally is lower than the expected values by as much as 40%. Figure 8A shows the rhodopsin dose response profiles obtained by measuring total [^{35}S]GTPγS binding or [γ-^{32}P]GTP hydrolysis, i.e., under conditions where [GTPγS] or [GTP] $\gg$ [α_T]. In this case, the simulations (Figure 8B) provide an excellent prediction for the total extent of rhodopsin-stimulated [^{35}S]GTPγS binding. These simulations also provide a good prediction of how the GTPase activity increases as a function of [rhodopsin], although in these experiments there is typically a 1.5–2-fold difference in the total amount of [^{32}P]P_i which is generated in GTPase assays compared to that predicted from the modeling. This difference is most likely due to a competition between the added GTP and the increasing amounts of GDP, which are being produced as an outcome of the continual GTP hydrolysis, for the rhodopsin–α_T complexes.

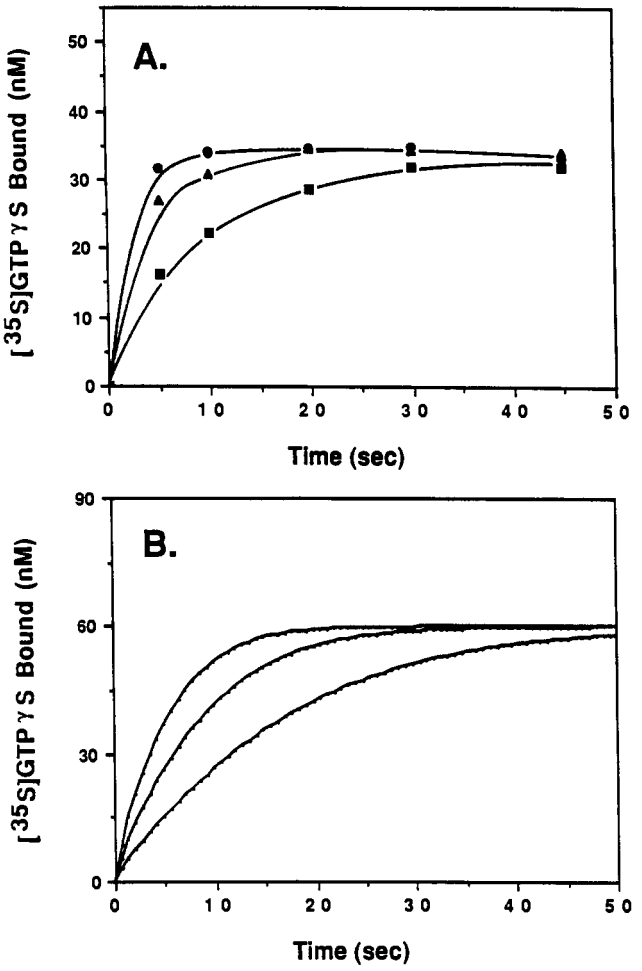

FIGURE 7: Rhodopin-stimulated GTPγS binding to the α_T subunit. (A) Rhodopsin-containing phosphatidylcholine vesicles, representing a final concentration of rhodopsin in the assay solution of 13 nM (■), 25 nM (▲), or 40 nM (●), were incubated with $\beta\gamma_T$ (67 nM), α_T (100 nM), and 60 nM [^{35}S]GTPγS at room temperature. At the time periods indicated, an aliquot (40 μL) was removed from the binding assay and applied to nitrocellulose filters to measure the amount of bound nucleotide (see Materials and Methods). (B) Simulations of [^{35}S]GTPγS binding for the conditions described in the legend for Figure 7A, using the model shown in Figure 5B and the best-fit parameters from the data shown in Figure 6.

For sake of simplicity, the model (Figure 5B) used to fit the fluorescence data does not account for this competition and thus would result in an overestimate in the predicted amount of [^{32}P]P_i release under conditions where high levels of GTP hydrolysis have occurred.

In the experiments shown in Figure 8A, as well as in all of the previous experiments described, the levels of rhodopsin in the assay incubation were varied by increasing the amounts of rhodopsin-containing phosphatidylcholine vesicles added to the assay solution. However, essentially identical rhodopsin dose response profiles were obtained when the levels of phospholipid vesicles were kept constant while varying the amount of rhodopsin per lipid vesicle (over a range from 1 to ≫10 rhodopsin molecules per lipid vesicle; data not shown). Thus, we find no indication that increasing the density of rhodopsin per lipid vesicle provides any advantage in terms of the rate or extent of transducin activation.

We also have found no indication that any of the kinetic parameters describing the rhodopsin-stimulated GTP (or GTPγS) binding to α_T, or the rhodopsin-stimulated GTP hydrolysis, are influenced by the lipid composition of our reconstituted system. Specifically, experiments measuring rhodopsin-stimulated guanine nucleotide binding or GTP

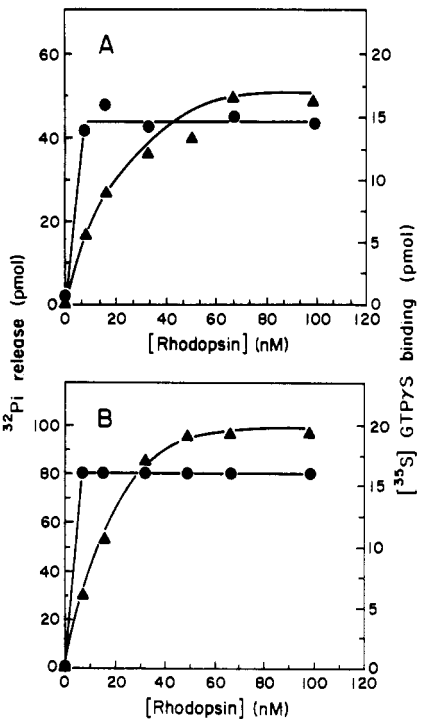

FIGURE 8: Simulations of the rhodopsin dose–response profiles for rhodopsin-stimulated [^{35}S]GTPγS binding and [γ-^{32}P]GTPase activity. (A) Rhodopsin-containing phosphatidylcholine vesicles (the final concentrations of rhodopsin are indicated in the figure), $\beta\gamma_T$ (final concentration = 70 nM), and α_T (~150 nM) were incubated in room light for 3 min when measuring [^{35}S]GTPγS binding (●) and for 10 min when measuring [γ-^{32}P]GTP hydrolysis (▲). These assays were performed by using 1 μM [γ-^{32}P]GTP or 1 μM [^{35}S]GTPγS as described under Materials and Methods. (B) Simulations of [^{35}S]-GTPγS binding and [γ-^{32}P]GTP hydrolysis for the conditions described in (A) using the model shown in Figure 5B and the best-fit parameters obtained from the data shown in Figure 6.

hydrolysis in liposomes prepared from a combination of phosphatidylcholine and a chloroform/methanol extract of rod outer segment lipids, or from liposomes that were prepared from rod outer segment lipids exclusively, yielded results identical with those obtained with liposomes prepared from soybean phosphatidylcholine (data not shown).

Discussion

The intrinsic tryptophan fluorescence of the α subunits of G proteins provides a potentially useful monitor for the GTP-binding–GTPase cycles of these transducer proteins. Previously, we have shown that changes in the intrinsic fluorescence of the α_T subunit can be clearly detected in response to rhodopsin-stimulated GTP binding (Phillips & Cerione, 1988). In this work, we have used these fluorescence changes to measure the kinetic parameters describing the activation and deactivation events for the retinal GTP-binding protein. The advantage of fluorescence approaches over other methods used to analyze G protein activation and deactivation, such as radiolabeled GTP-binding measurements or GTP hydrolysis assays, is that it enables the simultaneous monitoring of both binding and hydrolysis in real time. Thus, in principle, it should be possible to obtain the kinetic parameters describing the activation and deactivation events for transducin from a single trace of the GTP-induced fluorescence enhancement/decay sequence.

In order to establish the utility of this approach for kinetic analyses, we first set out to verify that the fluorescence enhancement and ensuing decay, which are elicited in a rhodopsin- (and $\beta\gamma_T$)-dependent manner upon the addition of

GTP, directly reflect the GTP-binding (GDP–GTP exchange) and GTP hydrolytic events. Direct comparisons of the GTP- and GTPγS-induced fluorescence enhancements suggested that the net fluorescence enhancements elicited by the addition of GTP actually represented a composite of the conformational changes which accompany GTP binding (enhancement) and GTP hydrolysis (fluorescence decay). Thus, when the levels of rhodopsin were relatively low (i.e., ≤15 nM), the rates of the rhodopsin-stimulated binding of GTP were comparable to the rates for GTP hydrolysis, and the initial enhancement in fluorescence was limited by the onset of the deactivation of the α_T subunit (and the accompanying attenuation of the α_T fluorescence). However, at higher levels of rhodopsin, the rates for the activation and deactivation events were clearly distinguishable, and the enhancement more directly reflected the GTP-binding event. Under conditions of high rhodopsin concentration and saturating levels of GTP (i.e., 10 μM), the fluorescence enhancement could be prolonged. This was consistent with the achievement of a steady state where all of the α_T was in the GTP-bound form. When GTPγS was substituted for GTP, the hydrolytic step was eliminated, and the GTPγS-induced fluorescence enhancement directly reflected the binding of this GTP analogue.

The integration of the GTP-induced fluorescence enhancement/decay sequence accurately predicted the rate of the rhodopsin-stimulated [γ-^{32}P]GTP hydrolysis (cf. Figure 4), which indicated that the fluorescence decay was coincident with the GTP hydrolysis event. At any point during the decay, the addition of GTP immediately restored the fluorescence to the initial enhanced state (see Figure 3). This implies that the release of P_i following GTP hydrolysis and also the ensuing rhodopsin-stimulated dissociation of the tightly bound GDP all occur within the time scale of (if not faster than) the actual hydrolytic event. If either of these events were significantly slower than the hydrolysis of GTP, there would be a measurable lag in the restoration of the activated state when rechallenging the α_T subunit, during its fluorescence decay, with GTP. Thus, an important implication from these studies is that the GTP hydrolytic event, rather than any secondary event such as P_i release or a slow ensuing conformational change, limits the rate of deactivation.

The fluorescence data, obtained at different levels of rhodopsin and GTP, were analyzed in the context of a simple model for the rhodopsin-stimulated GTP-binding–GTPase cycle of transducin. This scheme was developed along the lines of previous models proposed by Fung (1983) and Chabre (1985). In this scheme, rhodopsin initially couples to the GDP-bound α_T subunit (in the presence of $\beta\gamma_T$), which rapidly induces the dissociation of GDP. This in turn enables the binding of GTP, which is followed by a dissociation of the photoreceptor from the GTP-bound α_T species. Hence, a single receptor molecule can promote the activation of many α_T molecules. The principle assumptions in the modeling were that the dissociation of GDP from the rhodopsin–α_T(GDP) species was fast relative to the binding of GTP to the nucleotide-depleted rhodopsin–α_T species and that the association of rhodopsin with each α_T(GDP) molecule was fast relative to dissociation of the photoreceptor from the activated rhodopsin–α^*_T(GTP) complex. The former assumption was based on studies with the β-adrenergic receptor and the G_s protein which suggested that GDP dissociation was not rate-limiting for the hormone-stimulated binding of [^{35}S]GTPγS to G_s (Brandt & Ross, 1986). We feel that this assumption is a reasonable one for the rhodopsin/transducin system, since we have not observed a burst in the initial rate of GTP binding to α_T despite the fact that the α_T(GDP) was incubated with light-activated rhodopsin and $\beta\gamma_T$ for 10 min at room temperature prior to the start of the assay (i.e., conditions which should be sufficient to convert the α_T(GDP) to its nucleotide-depleted form). The assumption that the coupling of rhodopsin to the α_T(GDP) species is fast relative to the dissociation of the photoreceptor from the activated rhodopsin–α^*_T(GTP) species also seems reasonable based on our experimental data. Under conditions where [rhodopsin] < [α_T], the activation of the α_T(GDP) pool is limited either by the dissociation of a rhodopsin molecule from an activated rhodopsin–α^*_T(GTP) molecule or by the subsequent association of the receptor with another molecule of α_T(GDP). If this latter step were rate-limiting, it would be expected that as the levels of rhodopsin and α_T(GDP) were increased, the rates for the activation of the total α_T pool would increase. However, we have not found this to be the case; rather, we find that increasing the levels of both rhodopsin and the α_T(GDP) complex (while keeping the ratio of [rhodopsin] to [α_T(GDP)] essentially unchanged) does not change the rate of either the GTP-dependent activation or the GTPγS-dependent activation of α_T (data not shown). This, then, suggests that it is the first-order dissociation of the rhodopsin–α^*_T(GTP) species which limits the rate for the activation of the total α_T(GDP) pool when [α_T(GDP)] > [rhodopsin].

All of the fluorescence enhancement–decay sequences were fit well by a narrow range of parameters representing the rates for the GTP-binding event (k_{bind} = 0.005–0.007 nM^{-1} s^{-1}), the conversion of a rhodopsin–α_T(GTP) complex to a rhodopsin–α_T(GDP) complex (k_{exc} = 0.45–1.0 s^{-1}), and GTP hydrolysis ($k_{hyd} = k'_{hyd}$ = 0.034–0.040 s^{-1}). Thus, at [GTP] >10 nM, the hydrolysis of GTP is the rate-limiting step for the activation–deactivation cycle of transducin. The best-fit parameters for the fluorescence data provided good predictions for the rhodopsin dose response profiles for [^{35}S]GTPγS binding and [γ-^{32}P]GTP hydrolysis measurements (see Figures 7 and 8). It is worth noting that we find no differences in the types of rhodopsin dose response profiles obtained if the levels of rhodopsin are varied by simply adding increasing amounts of rhodopsin-containing vesicles to the assay solution or if the amount of rhodopsin molecules incorporated per lipid vesicle is increased (i.e., over a range of 1 to ≫10 rhodopsin molecules per lipid vesicle). A simple rhodopsin dose response profile is obtained in all cases with the rates for the GTP-binding event, and the measured turnovers for the GTP hydrolytic event, being comparable to those reported in other studies [Wessling-Resnick & Johnson, 1987b; Fung, 1983; also cf. Chabre (1985)]. Thus, we find no indication that the rhodopsin molecules need to act cooperatively to achieve the effective activation of α_T molecules. Previous indications of cooperativity may have been due to the oligomerization of the α_T subunits [cf. Wessling-Resnick and Johnson (1987b)].

Modeling of the fluorescence data sets an upper limit of 1–2 s for the release of rhodopsin from an activated α^*_T(GTP) species. This is significantly faster than GTP hydrolysis (~30 s) and thus is compatible with the finding that rhodopsin shows no direct effect on the rate of GTP hydrolysis. This is similar to the situation for the β-adrenergic receptor and the G_s protein, where Brandt and Ross (1986) suggested that the receptor does not affect the GTPase activity of G_s. The estimate for the rate of dissociation of rhodopsin from an activated α^*(GTP) molecule, suggested from these reconstitution studies, is similar to, although somewhat slower than, that proposed from light-scattering measurements made in rod outer segment membranes [i.e., it was suggested that about

eight rhodopsin–α_T(GTP) complexes dissociate per second; cf. Bennett and Dupont (1985)]. However, the rates for the activation of the total α_T pool obtained in our studies, under conditions where [α_T] $\gg$ [rhodopsin], are generally in good agreement with those obtained under similar conditions from direct binding measurements in rod outer segments (Bennett & Dupont, 1985).

The relationship between the rates for rhodopsin-stimulated GTP binding and the subsequent release of rhodopsin from an activated α_T subunit, to the overall extent of signal amplification in the visual transduction system, remains to be determined. It commonly has been suggested that the activation of a single rhodopsin molecule results in the hydrolysis of as many as 10^6 cyclic GMP molecules per second, which in turn suggests that at least 100 transducin molecules (per rhodopsin molecule) may participate in the signaling event [cf. Chabre (1985)]. Nonetheless, the results from the present study, as well as from the kinetic analyses of light-scattering data (Bennett & DuPont, 1985), which suggest that the dissociation of the rhodopsin–α^*_T(GTP) species may take 0.1–1 s, raise the possibility that the interaction of an activated α^*_T(GTP) species with the cyclic GMP PDE may occur prior to the release of rhodopsin from the GTP-bound α_T subunit. There, in fact, have been various prior suggestions that a receptor–G protein complex may stay intact at least until the activated G protein meets the effector. The initial postulation for the transient formation of a receptor–G protein–effector complex came from the kinetic studies of the hormone-stimulated adenylyl cyclase system by Levitzki and colleagues (Tolkovsky & Levitzki, 1978; Tolkovsky et al., 1982). A further suggestion for the existence of a receptor–α_s(GTP) species came from more recent reconstitution studies where the inhibition of adenylyl cyclase was being examined (Cerione et al., 1987). Specifically, the $\beta\gamma$ subunit complex was found to be less able to reassociate with an activated α_s species when the α_s was coupled to the β-adrenergic receptor compared to when the activated α_s was free in solution. Finally, a recent suggestion for the involvement of rhodopsin in the stimulatory interactions of transducin with the cyclic GMP phosphodiesterase comes from studies with a carboxyl-specific antibody against the α subunit of transducin [cf. Cerione et al. (1988) and Phillips et al. (1989)]. In these studies, it was shown that the antibody, designated as AS/7, markedly potentiated the ability of the activated α^*_T(GTPγS) species to stimulate the phosphodiesterase. Since the AS/7 binds to the same region on the α_T as rhodopsin, we have questioned whether rhodopsin may perform a similar function in directing the effective stimulation by transducin of cyclic GMP hydrolysis. In order to directly address this issue, future studies are being aimed at directly comparing the rate of dissociation of rhodopsin from the α_T(GTP) species to the rate for the interaction of an activated α_T subunit with the PDE by the use of fluorescence resonance energy transfer approaches where the receptor, the α_T subunit, and the PDE are labeled with extrinsic reporter groups.

Registry No. GTPase, 9059-32-9; GTP, 86-01-1; GDP, 146-91-8.

References

Avron, M. (1960) *Biochim. Biophys. Acta 40*, 257.

Baehr, W., Devlin, M. J., & Applebury, M. L. (1979) *J. Biol. Chem. 254*, 11669–11677.

Bennett, N., & Dupont, Y. (1985) *J. Biol. Chem. 260*, 4156–4168.

Berridge, M. J. (1987) *Annu. Rev. Biochem. 56*, 159–193.

Bradford, M. M. (1976) *Anal. Biochem. 72*, 248–254.

Brandt, D. R., & Ross, E. M. (1986) *J. Biol. Chem. 261*, 1656–1664.

Burch, R. M., Luini, A., & Axelrod, J. (1986) *Proc. Natl. Acad. Sci. U.S.A. 83*, 7201–7205.

Cerione, R. A., Staniszewski, C., Benovic, J. L., Lefkowitz, R. J., Caron, M. G., Gierschik, P., Somers, R., Spiegel, A. M., Codina, J., & Birnbaumer, L. (1985) *J. Biol. Chem. 260*, 1493–1500.

Cerione, R. A., Gierschik, P., Staniszewski, C., Benovic, J. L., Codina, J., Somers, R., Birnbaumer, L., Spiegel, A. M., Lefkowitz, R. J., & Caron, M. G. (1987) *Biochemistry 26*, 485–1491.

Cerione, R. A., Kroll, S., Rajaram, R., Unson, C., Goldsmith, P., & Spiegel, A. M. (1988) *J. Biol. Chem. 263*, 9345–9352.

Chabre, M. (1985) *Annu. Rev. Biophys. Chem. 14*, 331–360.

Dixon, R. A. F., Kobilka, B. K., Strader, D. J., Benovic, J. L., Dohlman, H. G., Frielle, T., Bolanowski, M. A., Bennett, C. D., Rands, E., Diehl, R. E., Mumford, R. A., Slater, E. E., Sigal, I. S., Caron, M. G., Lefkowitz, R. J., & Strader, C. D. (1986) *Nature 32*, 75–79.

Fung, B. K.-K. (1983) *J. Biol. Chem. 258*, 10495–10502.

Gierschik, P., Simons, C., Woodard, C., Somers, R., & Spiegel, A. (1984) *FEBS Lett. 172*, 321–325.

Gilman, A. G. (1987) *Annu. Rev. Biochem. 56*, 615–650.

Greenwood, F. C., Hunter, W. M., & Glover, J. S. (1963) *Biochem. J. 89*, 114–123.

Hargrave, P. A., McDowell, J. H., Curtis, D. R., Wang, J. K., Jusczak, E., Fong, L.-L., Rao, J. K. M., & Argos, P. (1983) *Biophys. Struct. Mech. 9*, 235–244.

Hescheler, J., Rosenthal, W., Trautwein, W., & Schultz, G. (1987) *Nature 325*, 445–447.

Higashijima, T., Ferguson, K. M., Sternweis, P. C., Ross, E. M., Smigel, M. D., & Gilman, A. G. (1987a) *J. Biol. Chem. 262*, 752–756.

Higashijima, T., Ferguson, K. M., Smigel, M. D., & Gilman, A. G. (1987b) *J. Biol. Chem. 262*, 757–761.

Kobilka, B. K., Matsui, H., Kobilka, T. S., Yang-Feng, T. L., Francke, U., Caron, M. G., Lefkowitz, R. J., & Regan, J. W. (1987) *Science 238*, 650–656.

Kohnken, R. E., Eadie, D. M., Revzin, A., & McConnell, D. G. (1981) *J. Biol. Chem. 256*, 12502–12509.

Kubo, T., Fukuda, K., Mikami, A., Maeda, A., Takahashi, H., Mishina, M., Haga, T., Haga, K., Ichiyama, A., Kanagawa, K., Kojima, M., Matsuo, H., Hirsoe, T., & Numa, S. (1986a) *Nature 321*, 75–79.

Kubo, T., Maeda, A., Sugimoto, K., Akiba, I., Mikami, A., Takahashi, H., Haga, T., Haga, K., Ichiyama, A., Kanagawa, K., Matsuo, H., Hirsoe, T., & Numa, S. (1986b) *FEBS Lett. 209*, 367–372.

Lefkowitz, R. J., & Caron, M. G. (1988) *J. Biol. Chem. 263*, 4993–4996.

Litman, B. J. (1982) *Methods Enzymol. 81*, 150–153.

Logothetis, D. E., Kurachi, Y., Galper, J., Neer, E. J., & Clapham, D. E. (1987) *Nature 325*, 321–326.

McCracken, D. D., & Dorn, W. S. (1964) *Numerical Methods and Fortran Programming*, Wiley, New York.

Nelder, J. A., & Mead, R. (1965) *Comput. J. 7*, 308–313.

Phillips, W. J., & Cerione, R. A. (1988) *J. Biol. Chem. 263*, 15498–15505.

Phillips, W. J., Trukawinski, S., & Cerione, R. A. (1989) *J. Biol. Chem. 264*, 16679–16688.

Pines, M., Gierschik, P., Milligan, G., Klee, W., & Spiegel, A. M. (1985) *Proc. Natl. Acad. Sci. U.S.A. 82*, 4095–4099.

Smith, C. D., Cox, C. C., & Snyderman, R. (1986) *Science 232*, 97–100.

Stryer, L., Hurley, J. B., & Fung, B. K.-K. (1981) *Curr. Top. Membr. Transp. 15*, 93-108.
Tolkovsky, A. M., & Levitzki, A. (1978) *Biochemistry 17*, 3795-3810.
Tolkovsky, A. M., Braun, S., & Levitzki, A. (1982) *Proc. Natl. Acad. Sci. U.S.A. 79*, 213-217.
Wessling-Resnick, M., & Johnson, G. L. (1987a) *J. Biol. Chem. 262*, 3697-3705.
Wessling-Resnick, M., & Johnson, G. L. (1987b) *J. Biol. Chem. 262*, 12444-12447.
Yatani, A., Codina, J., Brown, A. M., & Birnbaumer, L. (1987) *Science 235*, 207-211.

Structure, Multiple Site Binding, and Segmental Accommodation in Thymidylate Synthase on Binding dUMP and an Anti-Folate[†,‡]

William R. Montfort, Kathy M. Perry, Eric B. Fauman, Janet S. Finer-Moore, Gladys F. Maley,[§] Larry Hardy,[∥] Frank Maley,[§] and Robert M. Stroud*

Department of Biochemistry and Biophysics, S-960, University of California in San Francisco, San Francisco, California 94143-0448

Received November 20, 1989; Revised Manuscript Received March 22, 1990

ABSTRACT: The structure of *Escherichia coli* thymidylate synthase (TS) complexed with the substrate dUMP and an analogue of the cofactor methylenetetrahydrofolate was solved by multiple isomorphous replacement and refined at 1.97-Å resolution to a residual of 18% for all data (16% for data $>2\sigma$) for a highly constrained structure. All residues in the structure are clearly resolved and give a very high confidence in total correctness of the structure. The ternary complex directly suggests how methylation of dUMP takes place. C-6 of dUMP is covalently bound to γS of Cys-198(146) during catalysis, and the reactants are surrounded by specific hydrogen bonds and hydrophobic interactions from conserved residues. Comparison with the independently solved structure of unliganded TS reveals a large conformation change in the enzyme, which closes down to sequester the reactants and several highly ordered water molecules within a cavernous active center, away from bulk solvent. A second binding site for the quinazoline ring of the cofactor analogue was discovered by withholding addition of reducing agent during crystal storage. The chemical change in the protein is slight, and from difference density maps modification of sulfhydryls is not directly responsible for blockade of the primary site. The site, only partially overlapping with the primary site, is also surrounded by conserved residues and thus may play a functional role. The ligand-induced conformational change is not a domain shift but involves the segmental accommodation of several helices, β-strands, and loops that move as units against the β-sheet interface between monomers.

Thymidylate synthase (TS)[1] (EC 2.1.1.45) catalyzes the reductive methylation of deoxyuridine monophosphate (dUMP) by 5,10-methylenetetrahydrofolate (CH_2-H_4folate) to form thymidine monophosphate (dTMP) and dihydrofolate (H_2folate) (Figure 1) [reviewed by Pogolotti and Santi (1977)]. Conformation changes are associated with initial binding of dUMP (Galivan et al., 1975; Leary et al., 1975), with even larger changes accompanying binding of cofactor, evaluated both by spectroscopic (Sharma & Kisliuk, 1973; Danenberg et al., 1974; Santi et al., 1974; Donato et al., 1976) and by hydrodynamic methods. Gel filtration and sedimentation analyses show a large apparent decrease of 3.5% in Stokes radius of *Lactobacillus casei* and human protein in response to ternary complex formation (Lockshin & Danenberg, 1980). The structure of unliganded[2] TS from *L. casei* was solved first (Hardy et al., 1987). However, to describe these large structural changes and to help delineate their role in catalysis, we sought to determine the structure of a ternary complex of a close analogue of the normal TS·dUMP·CH_2-H_4folate complex that could be compared directly with the structure of the unliganded protein of the same species. We first crystallized such a pair of structures for this comparison with TS from *Escherichia coli*. The structure of the ternary complex reported here was solved and refined independently from the structure of unliganded *E. coli* TS (Perry et al., 1990), thus eliminating any bias in interpretation of conformational differences.

As TS is the terminal step in the sole de novo synthetic pathway to dTMP, it has, since the discovery of 5-fluorouracil

[†] Supported by National Institutes of Health Grants RO1-CA-41323 to J.S.F.-M. and R.M.S., GM24485 to R.M.S., and CA44355 to F.M., by NSF Grant DM386-16273 to G.F.M., and by postdoctoral fellowships from the American Chemical Society (S-49-87 to W.R.M.) and from NIH (GM-11846 to K.M.P.). E.B.F. is a Howard Hughes Medical Institute Predoctoral Fellow.

[‡] Crystallographic coordinates have been submitted to the Brookhaven Protein Data Bank under 1TSC,1TMS.

* Author to whom correspondence should be addressed.

[§] Present address: Wadsworth Center for Laboratories and Research, New York State Department of Health, Empire State Plaza, Albany, NY 12201-0509.

[∥] Present address: Department of Pharmacology, University of Massachusetts Medical School, Worcester, MA 01655.

[1] Abbreviations: TS, thymidylate synthase; dUMP, 2′-deoxyuridine 5′-monophosphate; CH_2-H_4folate, 5,10-methylenetetrahydrofolate; dTMP, thymidine 5′-monophosphate; H_2folate, dihydrofolate; CB3717, 10-propargyl-5,8-dideazafolate; MIR, multiple isomorphic replacement; R_{crys}, crystallographic R factor.

[2] Unliganded structures refer to structures with inorganic phosphate bound at the site for phosphate in dUMP.

0006-2960/90/0429-6964$02.50/0